Pergamon

Cement and Concrete Research, Vol. 26, No. 12, pp. 1789-1799, 1996

0008-8846/96 $15.00 + .00

PII S0008-8846(96)00174-3

STRENGTH, PORE STRUCTURE AND PERMEABILITY OF ALKALI-ACTIVATED SLAG MORTARS

Caijun Shi
Water Technology International Corporation
Operator of the Wastewater Technology Centre and the Canadian Clean Technology Centre
867 Lakeshore Road, P.O. Box 5068, Burlington, Ontario, Canada L7R 4L7

(Refereed)
(Received July 16, 1996; in final form October 15, 1996)

ABSTRACT

This paper deals with the strength development, pore structure development, rapid chloride permeability and water permeability of alkali-activated slag mortars activated by 6% (by mass of Na_2O) NaOH, Na_2CO_3 and Na_2SiO_3. The Na_2SiO_3-activated slag mortars exhibited the highest strength at both early and later ages, even much higher than a typical commercial Type III portland cement. NaOH-activated slag mortars exhibited the lowest strength. The pore structure measurements were consistent with strength results. Four common strength-porosity equations: Balshin's, Ryshkevitch's, Schiller's, and Hasselmann's equations, fit the experimental results from alkali-activated slag mortars with sufficient efficiency; of which Hasselmann's equation fit best. The charge passed through the mortar specimens in the rapid chloride ion permeability test appeared to be dependent more on the chemistry of pore solution than on the pore structure of the mortars. Limited results from water permeability testing appeared to be consistent with strength and pore structure measurements.

Introduction

In addition to the factors which affect the hydration and structure development of portland cement concrete, the nature and dosage of activators play a crucial role in determining the hydration and structure development of alkali-activated slag cement concrete [1-3]. Many researchers have noticed the selectivity of alkaline activators; i.e., the effect that an activator has on strength development may be different for slags of different origins [4, 5]. Matelepszy [4] has found that Na_2CO_3 is especially suitable for slags rich in C_2MS, and NaOH is a good activator for slags rich in C_2AS. Analysis of hydration chemistry has indicated that the selectivity of activators results from the difference in hydration products and microstructure [5]. In most cases, waterglass ($Na_2O.nSiO_2$) is the most effective activator. However, the optimum modulus (n) of waterglass also varies with slags. Shi et al [6, 7] has concluded that the optimum modulus is 1.5 for granulated phosphorus slag.

It is generally accepted that hardened alkali-activated slag cement pastes have a structure different from that portland cement pastes do. However, limited work has been done on

the relationships between strength, pore structure and permeability of alkali-activated slag cementing materials. This study investigated the strength development, pore structure development and permeability of NaOH, Na_2CO_3 and Na_2SiO_3-activated slag mortars.

Experimentation

Raw Materials. A ground pelletized Canadian blast furnace slag was used in this study, and a typical commercial ASTM Type III portland cement was used as a reference cement. Chemical composition and some physical properties of the slag and the portland cement are shown in Table 1.

Chemical reagents NaOH, Na_2CO_3 and $Na_2SiO_3.9H_2O$ were used as alkaline activators. The dosage of alkaline activator was 6% Na_2O (by mass) based on the mass of slag. These activators were dissolved into mixing water first and then added to the ground slag during the mortar mixing.

Preparation of Specimens. The mortar mixtures were prepared by following ASTM C109. A water to slag ratio of 0.485 was used for all batches. For each batch, 50 × 50 × 50 mm cubes were cast for compressive strength and mercury intrusion pore structure tests, 100 × 50 mm cylinders for the rapid chloride ion permeability test (ASTM C1202) and truncated cones for water permeability test. After 24 hours, all specimens were demoulded and cured in a fog room at 23°C until test ages. Water storage was avoided since water curing will leach out alkali activators in the specimens and reduce the activation effect.

Compressive Strength. Three cubes were taken out for compressive strength test (ASTM C109) at ages of 1, 3, 7, 28, 90 and 180 days. The strength reported was an average of three specimens.

TABLE 1

Chemical Composition and Physical Properties of Blast Furnace Slag and Portland Cement

Item	Blast Furnace Slag (mass %)	Portland Cement (mass %)
SiO_2	35.33	21.41
Al_2O_3	9.94	4.57
Fe_2O_3	0.62	3.02
CaO	34.65	60.80
MgO	14.63	4.18
SO_3	3.97	3.58
Na_2O	0.31	0.15
K_2O	0.44	0.92
LOI	0	1.60
Total	99.89	100.24
Density (kg/m^3)	2930	3160
Blaine Fineness (m^2/kg)	400	552

Rapid Chloride Ion Permeability Test. The rapid chloride ion permeability test was performed following ASTM C1202 [8]. Specimens were taken out from the fog room one day before the testing. The periphery of the specimens was dried with paper towels and coated with rapid setting epoxy resin to prevent drying of the specimens during the testing. The epoxy resin was allowed to harden for up to two hours. During this period, the bottom and top ends of the cylinders were covered with plexiglass. Specimens were then placed into deaerated water in a beaker and vacuum saturated for 6–8 hours until no visible air bubbles came out of the specimens. These vacuum saturated specimens were left in deaerated water until testing. The test was performed after 3, 7, 28 and 90 days of curing of the specimens.

Mercury Intrusion Porosimetry Test. At ages of 3, 7, 28 and 90 days, one mortar cube for each batch was broken into small fragments and then placed in a bath of liquid nitrogen. After 2–3 minutes in the bath, these fragments were carefully moved to a vacuum freeze-drying apparatus to remove all free water [9]. These dried fragments were stored in sealed containers for mercury porosimetry tests. The pressure was applied from zero to 240 MPa (35,000 psi). A constant contact angle of 140° and a constant surface tension of mercury of 480 mN/m were assumed for the pore size calculation.

Water Permeability Test. The specimens for water permeability test were cut to the proper shape with a size of 10 cm top diameter, 9.2 cm bottom diameter and 2.7 cm height during the curing period. Some specimens cracked during the cutting and intact specimens were placed back into the fog curing room. Specimens were taken out of the fog room one day before the testing and saturated in the same way as described for the rapid chloride permeability test.

The description of the water permeability testing apparatus and procedures can be found elsewhere [10]. After a specimen was sealed in the pressure cell, water under a pressure of 6.9 to 13.8 MPa (1000 to 2000 psi) was applied to one surface of the specimens. When steady-state flow was reached, the quantity of water flowing through the specimen in a given time was measured. The coefficient of permeability, K, is calculated as follows:

$$K = \frac{Q}{A\frac{H}{L}} \tag{1}$$

where:

Q = volume outflow rate (m^3/s);
A = cross-section area of the specimen (m^2);
H = water head (m);
L = height of the specimen (m).

Experimental Results

Compressive Strength. Figure 1 shows the compressive strength development of alkali-activated slag and portland cement mortars. The strength of alkali-activated slag mortars varied with activators. Among the four mortars, Na_2SiO_3-activated slag (NS) mortars gave the highest compressive strength at all testing ages, much higher than the Type III portland cement (PC(III)) mortars. Na_2CO_3 -activated slag (NC) mortars did not show a compressive

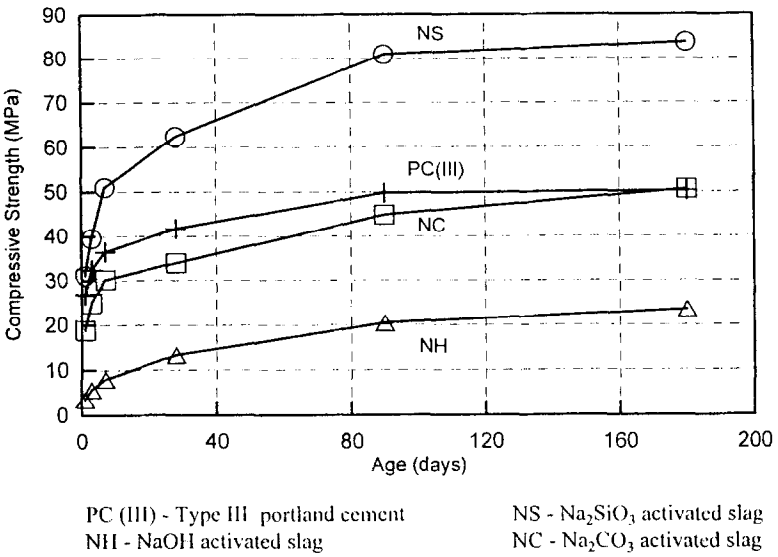

FIG. 1.
Strength development of alkali-activated slag and Portland cement mortars.

strength as high as the Type III portland cement at early ages, but an equivalent compressive strength at later ages. NaOH activated slag (NH) mortars exhibited the lowest compressive strength at all testing ages. The results described above indicated that Na_2SiO_3 was the most effective activator for the slag studied.

Pore Structure Characteristics. Figure 2 is the pore structure characteristics of PC(III) and alkali-activated slag mortars from 3 to 90 days. NS mortars (Fig. 2-b) exhibited a significantly lower measured porosity than the PC(III) mortars (Fig. 2-a). The porosity of 3-day old NS mortars was even lower than that of 90-day old PC(III) mortars. The other significant difference between the two mortars was the pore size distribution: PC(III) mortars had a continuous distribution over measured pore size range from 50 to 12,000 Å , while NS mortars contained only pores smaller than 100 and greater than 2000 Å. At a given age, NC mortars (Fig. 2-c) had a slightly lower porosity than PC(III) mortars. At 3 and 7 days, the cumulative pore volume decreased quickly with the increase in pore radius smaller than 1000 Å and the decrease trend slowed down thereafter. At 28 and 90 days, the pore size distribution of NC mortars was very similar to that of NS mortars: only pores smaller than 300 and larger than 2000 Å being measured. NH mortars (Fig. 2-d) had the highest porosity among the four mortars for a given age, and showed uniformly distributed pores over the measured pore size range.

Chloride Ion Permeability. Figure 3 is the charge passed through the specimens in the rapid chloride permeability test. NS and PC(III) mortars exhibited very high passed charges at 3 days. The charge passed through PC(III) mortars deceased significantly from 3 to 7 days, and no significant changes happened thereafter. The charge passed through NS mortars decreased significantly from 3 to 28 days, and remained almost a constant of 5000 coulombs

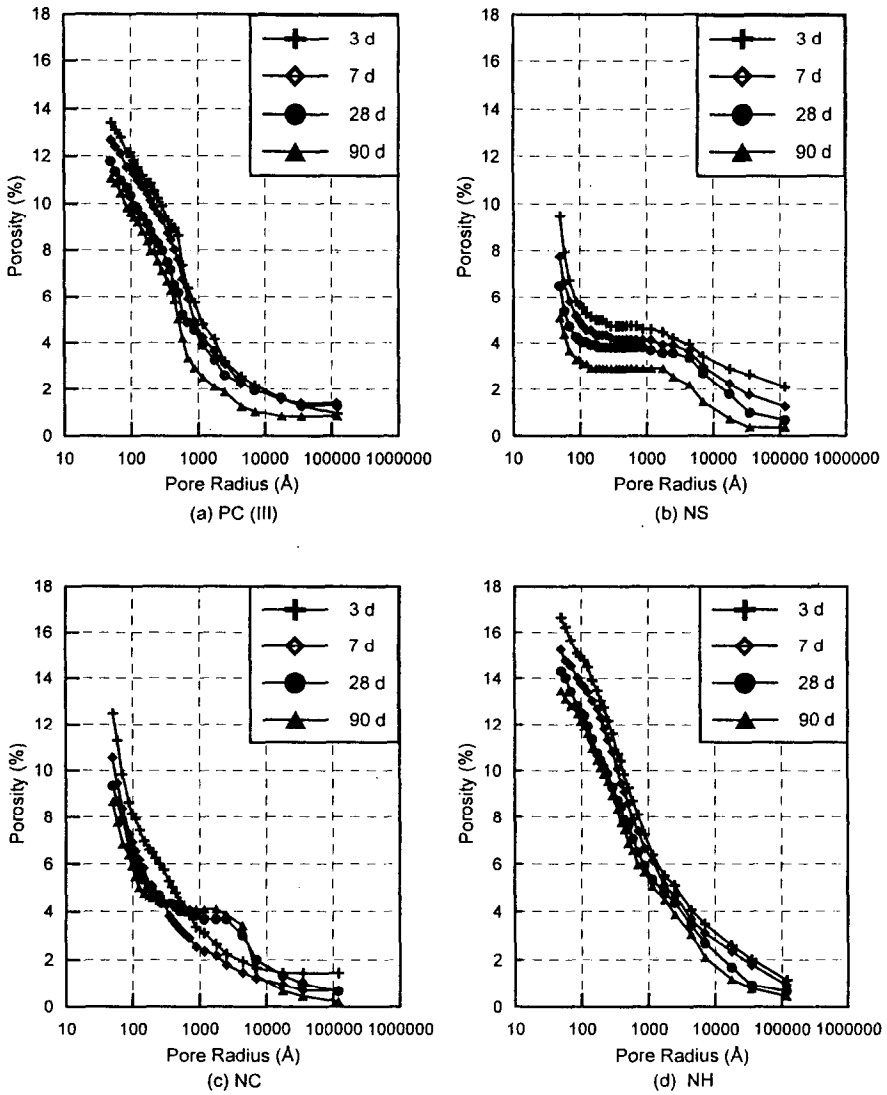

FIG. 2.
Cumulative pore volume of alkali-activated slag and Portland cement mortars.

thereafter. NC and NH mortars exhibited a very narrow range of the passed charge from 3 to 90 days: 2,000 to 3,000 coulombs.

Water Permeability. A limited amount of water permeability testing results were obtained because some specimens broke during cutting. The water permeability test results are plotted in Fig. 4. NS mortars showed the lowest while PC (III) mortars the highest water permeability at 7 days. No results were obtained from NH mortars.

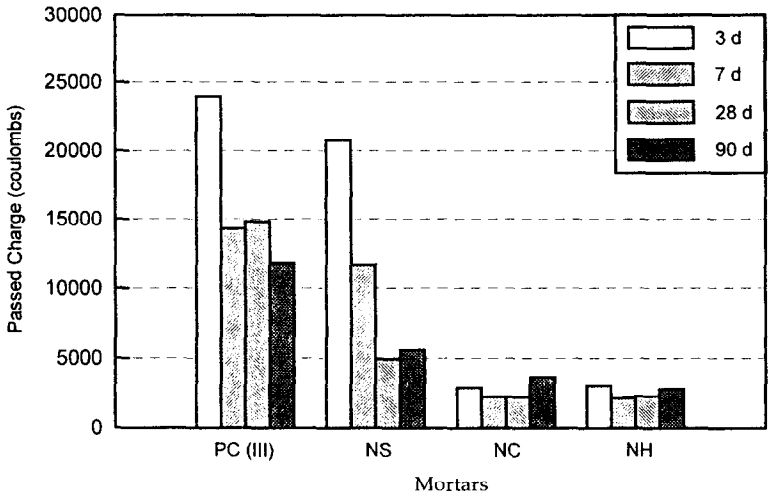

FIG. 3.
Chloride permeability of alkali-activated slag and portland cement mortars.

Discussion

Relationship Between Porosity and Compressive Strength. It is generally accepted that the pore structure plays an important role in determining the strength of hardened cement paste and concrete. The relationships between pore structure and strength have been summarized in previous publications [11, 12]. The pore size distribution, the shape and position of pores are also important, but it is both difficult and impractical to include all these parameters. Many experimental results have confirmed that an acceptable prediction of strength can be

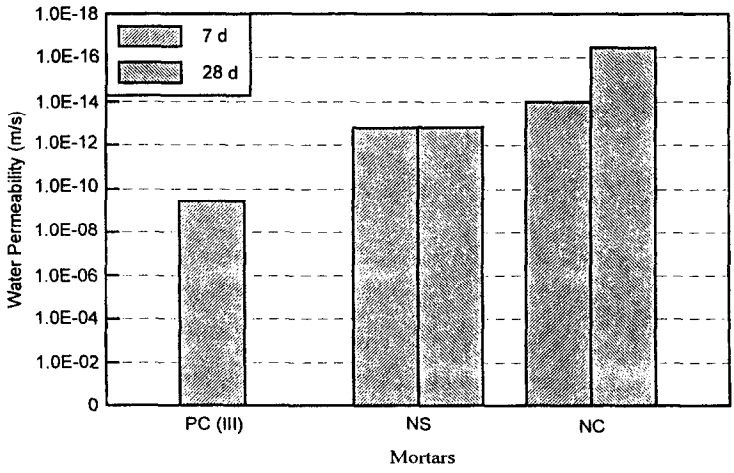

FIG. 4.
Water permeability of alkali-activated slag and portland cement mortars.

obtained by using total porosity. The most common relationships between porosity and compressive strength of portland cement pastes are [11, 12]:

Balshin's Equation:

$$\sigma = \sigma_o.(1 - P)^A \quad (1)$$

Ryshkevitch's Equation:

$$\sigma = \sigma_o.\exp(-BP) \quad (2)$$

Schiller's Equation:

$$\sigma = D.\ln(\frac{P_o}{P}) \quad (3)$$

and Hasselmann's Equation:

$$\sigma = \sigma_o.(1 - AP) \quad (4)$$

where:

σ_o - compressive strength at zero porosity;
P - porosity;
P_o - porosity at zero strength;
σ - compressive strength at porosity P;
A, B, D - experimental constants.

Most other relationships are variations of one of the four types. Equation (2) is especially suitable for low porosity systems and equation (3) for high porosity systems.

Robler and Odler [10] have examined a series of cement pastes with different water to cement ratios at different ages, and concluded that the existing relationships between strength and porosity within the common porosity range can be expressed with sufficient accuracy with by of the above equations, but Hasselmann's equation yields slightly more accurate results than others.

The relationships between compressive strength and the porosity ($r > 50$ Å) of alkali-activated slag and portland cement mortars are plotted in Fig. 5. It can be seen that all alkali-activated slag mortars, regardless of the nature of activator, follow the same trend, which is significantly different from that portland cement mortars follow. This may be explained by the similarity and difference in the nature of their main hydration product. Although the variation of activators changes the minor hydration products, the main hydration product of alkali-activated slag is always the same: C-S-H with a low C/S ratio [5]. While the main hydration product of portland cement is C-S-H with a high C/S ratio.

The four strength-porosity relationships, as described above, were used to depict the experimental results. The regression results by using SigmaPlot software are summarized in Table 2. The four equations yielded less accurate results for portland cement mortars than for alkali-activated slag mortars. The coefficients of variation of regression constants for alkali-activated slag mortars in the four equations ranged from 2.83 to 10.79%. Thus, all the four equations could depict the strength-porosity of alkali-activated slag mortars with sufficient accuracy. Hasselmann's equation showed the most accurate results for both portland cement and alkali-activated slag mortars.

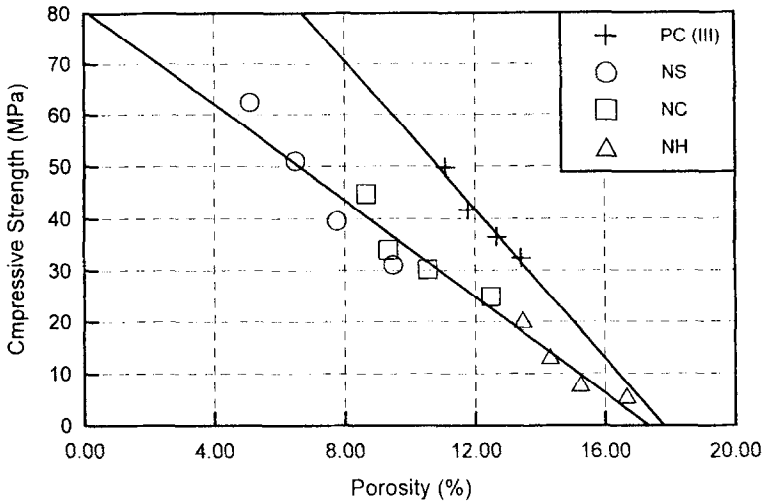

FIG. 5.
Relationship between porosity and strength of alkali-activated slag and portland cement mortars.

Pore Structure and Permeability. The rapid chloride ion permeability has been proposed to determine the permeability of a variety of concretes to chloride ions in a relatively short period of time [13]. The test method has been severely criticized because of its severe testing conditions which may cause both physical and chemical changes [14–17]. A recent work has indicated that the replacement of portland cement with supplementary cementing materials decreases the passed charges by more than 90% due to the change in pore solution composition which has little effect on the transport of chloride ions [18].

The results in Fig. 3 indicate the rapid chloride permeability test results in this study are contradictory to the pore structure characteristics of mortars. The explanations can be derived by plotting the initial current, which refers to the current recorded at the beginning of the test, and passed charge in coulombs, as shown in Fig. 6. The rapid chloride ion permeability test is essentially a measurement of electrical conductivity which depends on both the pore structure and the chemistry of pore solution. For a given specimen size and applied voltage, the recorded initial current can be regarded as a representative of electrical conductivity of the specimen. It can be seen that NS mortars exhibit higher electrical conductivity than NH or NC mortars. While the pore structure measurement has indicated that NS mortars are less porous than NH or NC mortars. Although the pore solutions were not analyzed, it is speculated that the chemistry of pore solution appears to contribute more to the electrical conductivity or the passed charge than the pore structure does in this study.

There is a good linear correlation between the initial current and the charge passed except for the two data from NS mortars at 3 and 7 days. The passed charge is the area underneath the recorded current (amperes) vs. time (from 0 to 21,600 seconds) curve. If the current does not change with time, the slope for the passed charge vs. initial current plot should be 21,600. The slope of 42566 in Fig. 6 indicated that a significant temperature rise

TABLE 2

Regression Results for the Strength-Porosity Relationship of Portland Cement and Alkali-Activated Slag Mortars

Mortar	Alkali-Activated Slag			Portland Cement		
Equation	Ryshkevitch's			$\sigma = \sigma_0 \cdot (1 - P)^4$		
Item	Value	Standard Error	Coefficient of Variation (%)	Value	Standard Error	Coefficient of Variation (%)
σ_0	131	13.41	10.03	326	65.02	19.97
A	13.83	1.16	8.39	16.15	1.56	9.69
Equation	Balshin's			$\sigma = \sigma_0 \cdot \exp(-B \cdot P)$		
σ_0	139	15.01	10.79	376	78.01	20.78
B	15.24	1.31	8.67	18.39	1.736	9.436
Equation	Schiller's Equation			$\sigma = D \cdot \ln(\frac{P_0}{P})$		
D	47.03	2.77	5.88	88.35	10.11	11.45
P_0	0.195	0.008	4.32	0.192	0.010	5.26
Equation	Hasselmann's			$\sigma = \sigma_0 \cdot (1 - AP)$		
σ_0	80.72	3.50	4.34	128.2	11.73	9.15
A	5.77	0.164	2.83	5.62	0.236	4.20

and structure change happened during the test. NS mortars show an lower initial current but a higher passed charge than PC(III) mortars at 3 and 7 days. It was found that the temperature of NS mortars after 3 and 7 days of curing rose more significantly than PC(III) mortars during the rapid chloride permeability test. The deviation of the two points far from the regressed straight line is attributed to the quick elevation of temperature of NS specimens which results in the quick increase of recorded current since the electrical conduction of mortars depends on the movement of ions. Thus, both the variation of pore solution composition and elevation of temperature significantly affect the rapid chloride permeability test results

Many models and theories [19–21] have been proposed to correlate water permeability and pore structure parameters, such as porosity, pore surface area, hydraulic mean radius, critical pore radius and porosity larger than some arbitrary pore size, of hardened cement and concrete. In this study, limited tests were conducted on hardened mortars and no attempts were made to correlate the pore structure characteristics and water permeability. However, a general trend can be observed that the lower the porosity and the finer the pore structure, the lower the water permeability.

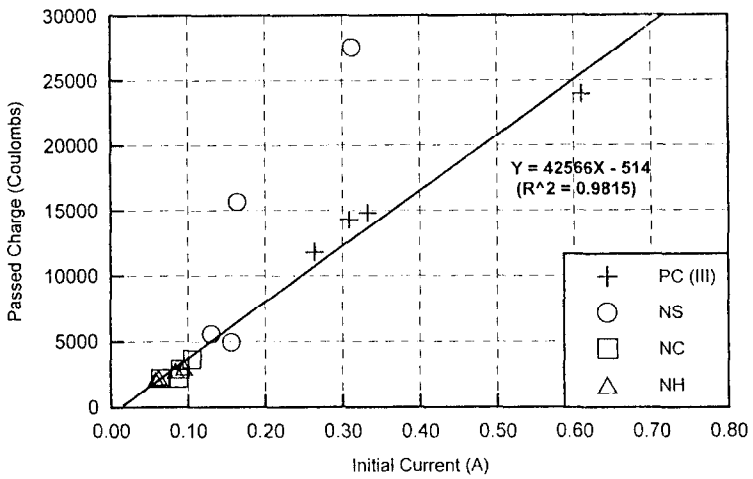

FIG. 6.
Relationship between initial current and passed charge.

Conclusions

This study has used different characterization techniques to test alkali-activated slag mortars and used established theories to correlate or to explain the experimental results. The following conclusions can be drawn:

(1) Na_2SiO_3 was the most effective activator among NaOH, Na_2CO_3 and Na_2SiO_3, for the studied slag. Na_2SiO_3-activated slag mortars gave much higher strength than Type III portland cement at both early and later ages.

(2) The pore structure characteristics of alkali-activated slag mortars varied with alkaline activators. Na_2SiO_3-activated slag mortars exhibited the lowest porosity and finest pore structure, and NaOH-activated slag mortars the highest porosity and coarsest pore structure.

(3) The strength-porosity relationship of alkali-slag mortars could be expressed with sufficient accuracy by Balshin's, Ryshkewitch's, Schiller's and Hasselmann's equations, of which Hasselmann's equation produced the most accurate results. While the four equations yielded less accurate results for portland cement mortars than for alkali-activated slag mortars. Based on the relationship between strength and porosity, the strength difference of different alkali-activated cementing materials was attributed to the differences in pore structure of hardened mortars.

(4) The rapid chloride ion permeability test is essentially a measurement of electrical conductivity and depends on both the chemistry of pore solution and the pore structure characteristics of tested specimens. Although the pore solutions were not analyzed, it is speculated that the chemistry of pore solution appears to contribute more than the pore structure to the rapid chloride permeability test results. Also temperature elevation of the specimen has a very significant effect rapid chloride permeability test results.

References

1. C. Shi and R.L. Day, Cement and Concrete Research, Vol. 26, No.3, pp.439-448, 1996.
2. C. Shi and R.L. Day, Cement and Concrete Research, Vol. 25, No.6, pp.1333-1346, 1995.
3. C. Shi, R.L. Day, X. Wu and M. Tang, M., Proceedings of 9th International Congress on the Chemistry of Cements, Vol. 3, pp. 298-304, New Delhi, India, 1992.
4. J. Matolepszy, Proceedings of 8th International Congress on the Chemistry of Cements, Vol. IV, pp.104-107, Brazil, 1986.
5. C. Shi and R.L. Day, Cement, Concrete and Aggregate, Vol.18, No.1, pp. 8-14, June 1996.
6. C. Shi and Y. Li, IL Cemento, Vol.86, No.3, pp. 161-168, 1989.
7. C. Shi and Y. Li, Cement and Concrete Research, Vol.19, No.4, pp. 527-533, 1989.
8. ASTM C1202, Electrical Indication of Concrete's Ability to Resist Chloride Ion Penetration, Annual Book of American Society for Testing Materials Standards, Vol.C04.02, 1993.
9. D.M.F. Orr, Cement and Concrete Research, Vol.13, No.1, pp.146-148, 1983.
10. L. Konnecy, Relationship Between Strength, Permeability and Microstructural Characteristics of Blended Mortars, M. Sc. Thesis, The University of Calgary, Calgary, Canada, 1987.
11. I. Odler, Materials and Structure, Vol. 24, pp.143-157, 1991
12. M. Robler and I. Odler, Cement and Concrete Research, Vol.15, No.2, pp.320-330, 1985.
13. D. Whiting, Rapid Determination of the Chloride Permeability of Concrete, Research Report FHWA/RD-81/119, 1981.
14. C. Andrade, Cement and Concrete Research, Vol. 23, No.5, pp. 724-742, 1993.
15. R.F.Feldman, G.W. Chan, R.J. Brousseau and P.J. Tumidajski, ACI Materials Journal, Vol.91, No. 3, pp. 246-255, 1994.
16. P.E. Streicher and M.G. Alexander, Proceedings of the third CANMET/ACI International Conference on Durability of Concrete, Supplementary Papers, pp. 517-530, Nice, France, 1994.
17. D. Pfeifer, D. McDonald and P. Krauss, PCI Journal, January-February, pp. 38-47, 1994.
18. C. Shi, J.A. Stegemann and R.J. Caldwell, Effect of Supplementary Cementing Materials on the Rapid Chloride Permeability Test (AASHTO T 277 AND ASTM C1202) Results, to be published.
19. D.C. Hughes, Magazine of Concrete Research, Vol.37, No.133, pp. 227-233, 1985.
20. B.K. Nyame and J. M. Illston, Proceedings of 7th International Congress on the Chemistry of Cement, Vol. III, pp. VI.181-186, Paris, 1980.
21. A.J. Katz and A.H. Thompson, Physics Review B, Vol.34, No.11, pp. 8719-8181, 1986.